Int. J. Heat Mass Transfer. Vol. 36, No. 7, pp. 1819–1825, 1993
Printed in Great Britain

0017–9310/93 $6.00+0.00

Mixed convection along a nonisothermal vertical flat plate embedded in a porous medium: the entire regime

J. C. HSIEH, T. S. CHEN and B. F. ARMALY
Department of Mechanical and Aerospace Engineering and Engineering Mechanics, University of Missouri-Rolla, Rolla, MO 65401, U.S.A.

(*Received* 1 *April* 1992 *and in final form* 5 *August* 1992)

Abstract—The problem of mixed convection about a vertical flat plate embedded in a porous medium is analyzed. Nonsimilarity solutions are obtained for the cases of variable wall temperature (VWT) in the form $T_w(x) = T_\infty + ax^n$ and variable surface heat flux (VHF) in the form $q_w(x) = bx^m$. The entire mixed convection regime is covered by two different nonsimilarity parameters $\chi = [1+(Ra_x/Pe_x)^{1/2}]^{-1}$ and $\chi^* = [1+(Ra_x^*/Pe_x^{3/2})^{1/3}]^{-1}$, respectively, for VWT and VHF cases, from pure forced convection ($\chi = 1$ or $\chi^* = 1$) to pure free convection ($\chi = 0$ or $\chi^* = 0$). A finite-difference scheme was used to solve the system of transformed governing equations. Velocity and temperature profiles, and local Nusselt numbers are presented. It is found that as χ or χ^* decreases from 1 to 0, the thermal boundary layer thickness increases first and then decreases, but the local Nusselt number in the form $Nu_x(Pe_x^{1/2}+Ra_x^{1/2})^{-1}$ or $Nu_x(Pe_x^{1/2}+Ra_x^{*1/3})^{-1}$ decreases first and then increases. The correlation equations for the local and average Nusselt numbers are also obtained for the two surface heating conditions.

INTRODUCTION

THE STUDY of natural or mixed convection boundary-layer flow along an impermeable surface embedded in fluid-saturated porous media has received much attention in recent years. Many of the studies [1–5] were based on Darcy's law which neglects the viscous force acting on the impermeable surface and does not take into account the non-slip boundary condition at the wall. From the work of Hong *et al.* [6], the non-slip wall effect is found to decrease with increasing distance downstream of the leading edge and to be negligible for low-porosity media. On the other hand, because the non-slip boundary condition has a lesser effect on heat transfer rate than it does on the velocity field [7], Darcy's model is still acceptable, especially when the flow velocity is low [6] and the heat transfer is of interest.

Most of the published results are limited to situations in which similarity solutions exist [1, 2]. A general similarity transformation for mixed convection flow in a porous medium was reported by Nakayama and Koyama [8] for different types of geometries. However, the flow and thermal fields in mixed convection from surfaces in a porous medium are nonsimilar in nature. Nakayama and Pop [9] proposed a unified similarity transformation to cover all possible similarity solutions for free, forced, and mixed convection within Darcy and non-Darcy porous media, but the cases they considered for solution were restricted to the local similarity approximation. Nonsimilarity solutions for mixed convection about a nonisothermal horizontal cylinder and sphere embedded in a porous medium are reported by Minkowycz *et al.* [10] who employed the local nonsimilarity method of solution to obtain numerical results which were compared with those obtained from the local similarity solution. A deviation of 10–15% in the results between the two sets of solutions were reported. Hsieh *et al.* [11] reported nonsimilarity solutions for the problem of mixed convection along a vertical flat plate embedded in a porous medium by dividing the entire mixed convection regime into two regions; one covers the forced convection dominated regime and the other covers the free convection dominated regime. Two different nonsimilarity parameters were found to characterize the two separate regions.

The aim of the present work is to study mixed convection from a vertical flat plate embedded in a porous medium by introducing a single nonsimilarity parameter which covers the entire regime of mixed convection. Two surface heating conditions are considered: power-law variation of the wall temperature and power-law variation of the surface heat flux. In the former heating condition, the nonsimilarity parameter $\chi = [1+(Ra_x/Pe_x)^{1/2}]^{-1}$, which varies from one for pure forced convection to zero for pure free convection, is introduced. In the latter, the nonsimilarity parameter $\chi^* = [1+(Ra_x^*/Pe_x^{3/2})^{1/3}]^{-1}$, which also varies from one for pure forced convection to zero for pure free convection, is introduced. Numerical results were obtained by using a finite-difference scheme to solve the transformed systems of

NOMENCLATURE

f	dimensionless stream function for the case of VWT
F	dimensionless stream function for the case of VHF
$h(x)$	local heat transfer coefficient
$\bar{h}$	average heat transfer coefficient $(1/L)\int_0^L h(x)\,dx$
k	thermal conductivity
K	permeability coefficient of the porous medium
L	length of the plate
Nu_x	local Nusselt number, hx/k
$\overline{Nu}$	average Nusselt number, $\bar{h}L/k$
Pe_x	local Peclet number, $u_\infty x/\alpha$
q_w	local surface heat flux
Ra_x	local Rayleigh number for the VWT case, $g\beta[T_w(x)-T_\infty]Kx/(\nu\alpha)$
Ra_x^*	local Rayleigh number for the VHF case, $g\beta q_w(x)Kx^2/(k\nu\alpha)$
T	temperature
T_∞	free stream temperature
T_w	wall temperature
u, v	velocity components in x- and y-direction
u_∞	free stream velocity
x, y	axial and normal coordinates.

Greek symbols

α	effective thermal diffusivity of saturated porous medium
β	volumetric coefficient of thermal expansion
δ	boundary layer thickness
η	pseudo-similarity variable for the VWT case
η^*	pseudo-similarity variable for the VHF case
η_∞	value of η at the edge of boundary layer
θ	dimensionless temperature for the VWT case
Θ	dimensionless temperature for the VHF case
μ	dynamic viscosity
ν	kinematic viscosity
ρ	fluid density
τ_w	local wall shear stress
χ	nonsimilarity parameter for the VWT case
χ^*	nonsimilarity parameter for the VHF case
ψ	stream function.

Subscripts

f	forced convection dominated condition
n	free convection dominated condition.

equations. Correlation equations for the local and average Nusselt numbers are also presented.

ANALYSIS

Consider the problem of mixed convection along a heated vertical flat plate embedded in a saturated porous medium. The axial and normal coordinates are x and y, and the gravitational acceleration g is acting downward in the direction opposite to the x coordinate. The surface of the plate is subjected to a power-law variation in wall temperature, $T_w(x)$, or wall heat flux, $q_w(x)$. Fluid properties are assumed to be constant except for variations in density, and the porous medium is treated as isotropic. In addition, the flow velocity and the pores of the porous medium are assumed to be small for the Darcy's model to be valid [6]. With these assumptions and the application of the Boussinesq and boundary layer approximations, the governing system of conservation equations can be written as [4]

$$\frac{\partial u}{\partial x}+\frac{\partial v}{\partial y}=0 \tag{1}$$

$$\frac{\partial^2\psi}{\partial y^2}=\frac{K}{\mu}\rho g\beta\frac{\partial T}{\partial y} \tag{2}$$

$$\alpha\frac{\partial^2 T}{\partial y^2}=u\frac{\partial T}{\partial x}+v\frac{\partial T}{\partial y}. \tag{3}$$

In the equations above, the stream function ψ satisfies the continuity equation (1) with $u=\partial\psi/\partial y$ and $v=-\partial\psi/\partial x$, where u and v are Darcy's velocities in the x and y directions; T is the temperature; ρ, μ and β are the density, dynamic viscosity and thermal expansion coefficient of the fluid; and K and α are, respectively, the permeability and equivalent thermal diffusivity of the porous medium.

The boundary conditions for the present problem are

$$v=0,\quad T=T_w(x)=T_\infty+ax^n \quad \text{or}$$
$$q_w=-k(\partial T/\partial y)_{y=0}=bx^m \quad \text{at } y=0,$$
$$u\to u_\infty,\quad T\to T_\infty \quad \text{as } y\to\infty \tag{4}$$

where a, b, n and m are prescribed constants. It is noted here that the case of uniform wall temperature corresponds to $n=0$, whereas that of uniform surface heat flux to $m=0$. The next step is to transform the

system of equations (2)–(4) into a dimensionless form, separately for the case of power-law wall temperature variation and the case of power-law surface heat flux variation.

A. *Power-law variation of wall temperature*, $T_w(x) = T_\infty + ax^n$

In this case the following dimensionless nonsimilarity variables are introduced:

$$\eta = \frac{y}{x} Pe_x^{1/2}\, \chi^{-1} \tag{5}$$

$$\psi = \alpha\, Pe_x^{1/2}\, \chi^{-1} f(\chi, \eta), \quad \theta(\chi, \eta) = \frac{T - T_\infty}{T_w(x) - T_\infty} \tag{6}$$

$$\chi = \left[1 + \left(\frac{Ra_x}{Pe_x}\right)^{1/2}\right]^{-1} \tag{7}$$

where $Pe_x = u_\infty x/\alpha$ is the local Peclet number, $Ra_x = g\beta[T_w(x) - T_\infty]Kx/\nu\alpha$ is the local Rayleigh number, and χ is the nonsimilarity mixed convection parameter.

Substituting equations (5)–(7) into equations (2)–(4), one can obtain the following system of equations:

$$f''' = (1-\chi)^2\theta' \tag{8}$$

$$\theta'' + \tfrac{1}{2}[1 + n(1-\chi)]f\theta' - nf'\theta = \tfrac{1}{2}n\chi(1-\chi)\left(\theta'\frac{\partial f}{\partial \chi} - f'\frac{\partial \theta}{\partial \chi}\right) \tag{9}$$

with the boundary conditions

$$[1 + n(1-\chi)]f(\chi, 0) - n\chi(1-\chi)\frac{\partial f}{\partial \chi}(\chi, 0) = 0$$

$$\text{or } f(\chi, 0) = 0, \quad \theta(\chi, 0) = 1$$

$$f'(\chi, \infty) = \chi^2, \quad \theta(\chi, \infty) = 0. \tag{10}$$

The primes in equations (8)–(10) denote partial differentiations with respect to η.

The physical quantities of interest include the velocity components u and v, the wall shear stress τ_w, defined as $\tau_w = \mu(\partial u/\partial y)_{y=0}$, and the local Nusselt number $Nu_x = hx/k$, where $h = q_w/[T_w(x) - T_\infty]$. They are given by

$$u = u_\infty \chi^{-2} f' \tag{11}$$

$$v = -\left(\frac{\alpha}{x}\right) Pe_x^{1/2}\, \chi^{-1}\left\{\frac{1}{2}[1 + n(1-\chi)]f - \frac{1}{2}[1 - n(1-\chi)]\eta f' - \frac{1}{2}n\chi(1-\chi)\frac{\partial f}{\partial \chi}\right\} \tag{12}$$

$$\tau_w\left(\frac{x^2}{\mu\alpha}\right)(Pe_x^{1/2} + Ra_x^{1/2})^{-3} = f''(\chi, 0) \tag{13}$$

$$Nu_x(Pe_x^{1/2} + Ra_x^{1/2})^{-1} = -\theta'(\chi, 0). \tag{14}$$

The average Nusselt number $\overline{Nu}$ can be evaluated by finding the average heat transfer coefficient $\bar{h}$ from the local Nusselt number expression, equation (14). The final expression is

$$\overline{Nu} = \frac{2}{n} Pe_L^{1/2}\left(\frac{\chi_L}{1-\chi_L}\right)^{1/n} \times \int_{\chi_L}^{1} [-\theta'(\chi, 0)]\chi^{-3}\left(\frac{1-\chi}{\chi}\right)^{(1-n)/n} d\chi \tag{15}$$

where Pe_L and χ_L are values of Pe_x and χ at $x = L$. For the case of uniform wall temperature (i.e. $n = 0$), the corresponding average Nusselt number expression can be written as

$$[\overline{Nu}]_{n=0} = 2Pe_L^{1/2}\, \chi_L^{-1}[-\theta'(\chi_L, 0)]. \tag{16}$$

B. *Power-law variation of surface heat flux*, $q_w(x) = bx^m$

For this case, one introduces the following dimensionless variables:

$$\eta^* = \frac{y}{x} Pe_x^{1/2}\, \chi^{*-1} \tag{17}$$

$$\psi = \alpha\, Pe_x^{1/2}\, \chi^{*-1} F(\chi^*, \eta^*),$$

$$\Theta(\chi^*, \eta^*) = \frac{(T - T_\infty)Pe_x^{1/2}\, \chi^{*-1}}{q_w(x)x/k} \tag{18}$$

$$\chi^* = \left[1 + \left(\frac{Ra_x^*}{Pe_x^{3/2}}\right)^{1/3}\right]^{-1} \tag{19}$$

where $Ra_x^* = g\beta q_w(x)Kx^2/k\nu\alpha$ denotes the Rayleigh number and χ^* the nonsimilarity mixed convection parameter.

The transformation of equations (2)–(4) yields

$$F''' = (1-\chi^*)^3\Theta' \tag{20}$$

$$\Theta'' + \frac{1}{2}\left[1 + \frac{2}{3}\left(m + \frac{1}{2}\right)(1-\chi^*)\right]F\Theta' - \left(m + \frac{1}{2}\right)\left[1 - \frac{1}{3}(1-\chi^*)\right]F'\Theta = \frac{1}{3}\left(m + \frac{1}{2}\right)\chi^*(1-\chi^*)\left(\Theta'\frac{\partial F}{\partial \chi^*} - F'\frac{\partial \Theta}{\partial \chi^*}\right) \tag{21}$$

$$\frac{1}{2}\left[1 + \frac{2}{3}\left(m + \frac{1}{2}\right)(1-\chi^*)\right]F(\chi^*, 0) - \frac{1}{3}\left(m + \frac{1}{2}\right)\chi^*(1-\chi^*)\frac{\partial F}{\partial \chi^*}(\chi^*, 0) = 0$$

$$\text{or } F(\chi^*, 0) = 0, \quad \Theta'(\chi^*, 0) = -1$$

$$F'(\chi^*, \infty) = \chi^{*2}, \quad \Theta(\chi^*, \infty) = 0 \tag{22}$$

where the primes denote partial differentiations with respect to η^*.

The velocity components u and v, the wall shear stress and the local Nusselt number for this case have the expressions

$$u = u_\infty \chi^{*-2} F' \tag{23}$$

$$v = -\left(\frac{\alpha}{x}\right) Pe_x^{1/2}\, \chi^{*-1} \left\{\left[\frac{1}{2} + \frac{1}{3}\left(m+\frac{1}{2}\right)(1-\chi^*)\right]F - \left[\frac{1}{2} - \frac{1}{3}\left(m+\frac{1}{2}\right)(1-\chi^*)\right]\eta^* F' - \frac{1}{3}\left(m+\frac{1}{2}\right)\chi^*(1-\chi^*)\frac{\partial F}{\partial \chi^*}\right\} \tag{24}$$

$$\tau_w \left(\frac{x^2}{\mu\alpha}\right)(Pe_x^{1/2} + Ra_x^{*1/3})^{-3} = F''(\chi^*, 0) \tag{25}$$

$$Nu_x (Pe_x^{1/2} + Ra_x^{*1/3})^{-1} = \frac{1}{\Theta(\chi^*, 0)}. \tag{26}$$

The average Nusselt number $\overline{Nu}$ can be expressed as

$$\overline{Nu} = \frac{6}{2m+1} Pe_L^{1/2} \left(\frac{\chi_L^*}{1-\chi_L^*}\right)^{3/(2m+1)} \times \int_{\chi_L^*}^{1} \frac{\chi^{*-3}}{\Theta(\chi^*, 0)} \left(\frac{1-\chi^*}{\chi^*}\right)^{(2-2m)/(2m+1)} d\chi^* \tag{27}$$

where Pe_L and χ_L^* are values of Pe_x and χ^* at $x = L$. For the case of uniform wall temperature (i.e. $m = -0.5$), the corresponding expression is

$$[\overline{Nu}]_{m=-0.5} = \frac{2 Pe_L^{1/2}\, \chi_L^{*-1}}{\Theta(\chi_L^*, 0)}. \tag{28}$$

The two systems of equations, equations (8)–(10) and (20)–(22) for the VWT and VHF cases, respectively, can be solved using a finite-difference method as described by Cebeci and Bradshaw [12]. In this method, the partial differential equations (8)–(9) or (20)–(21) are first reduced to a system of first-order ordinary differential equations which are then expressed in finite-difference form and solved, along with their boundary conditions, by an iterative scheme. To conserve space, the details of the solution procedure are not represented here. It suffices to mention that a step size of $\Delta\eta = 0.02$ and η_∞ values of 8–18 were found to provide accurate numerical results.

RESULTS AND DISCUSSION

Numerical results were obtained for the two cases of VWT and VHF. They cover the values of exponents $0 \leqslant n \leqslant 1$ and $-0.5 \leqslant m \leqslant 1$. These exponent values are found to provide physically realistic problems, respectively, for the VWT and VHF cases. Following the argument used by Cheng and Minkowycz [3], the criterion in determining the range of n or m values is based on the requirements that both u and δ, the streamwise velocity component and the boundary layer thickness, respectively, must increase or at least remain constant with respect to x. From equations (5) and (17), it can be found that δ varies with $x^{(1-n)/2}$ or $x^{(1-m)/3}$ for pure free convection. Also from equations (6) and (18) the streamwise velocity u varies with x^n or $x^{(2m+1)/3}$ for pure free convection. Thus, the ranges of exponents n and m are $0 \leqslant n \leqslant 1$ and $-0.5 \leqslant m \leqslant 1$, respectively.

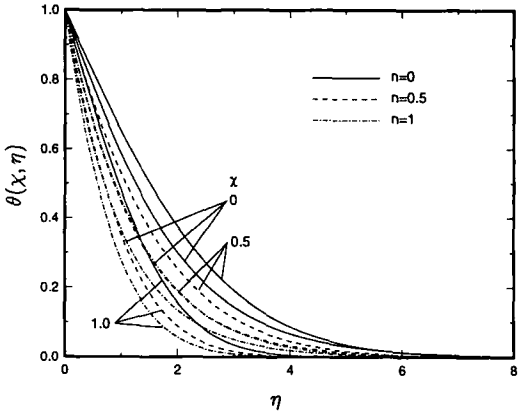

FIG. 1. Dimensionless temperature profiles at selected values of χ and n (VWT case).

A. *Power-law variation of wall temperature*

Figure 1 shows the dimensionless temperature profiles $\theta(\chi, \eta)$ at selected values of χ and n. It can be seen from the figure that, for a given value of χ, as n increases the thermal boundary layer thickness decreases and the temperature gradient at the wall increases. This means that a higher value of the heat transfer rate is associated with a higher value of n. Also, for a given value of n, the thermal boundary-layer thickness increases (with decreasing wall temperature gradient) as χ decreases from 1, reaching a maximum value at a certain χ value, and then decreases (with increasing wall temperature gradient) as χ decreases further to 0. Dimensionless velocity profiles in terms of $f'(\chi, \eta)$ are shown in Fig. 2. It can be seen that at a given χ value, the velocity gradient at the wall increases and the momentum boundary layer thickness decreases as n increases.

Values of $-\theta'(\chi, 0)$ at selected values of χ are presented in Table 1 for different n values. Figure 3 shows the local Nusselt number in terms of $Nu_x(Pe_x^{1/2} + Ra_x^{1/2})^{-1}$, or $-\theta'(\chi, 0)$, for selected exponent values

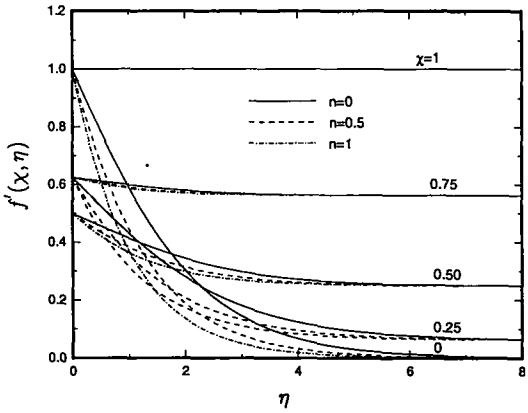

FIG. 2. Dimensionless velocity profiles $f'(\chi, \eta)$ at selected values of χ and n (VWT case).

Table 1. Values of $-\theta'(\chi, 0)$ and $1/\Theta(\chi^*, 0)$ at selected values of χ, n and χ^*, m

	$-\theta'(\chi, 0)$			$1/\Theta(\chi^*, 0)$			
χ or χ^*	$n = 0$	$n = 0.5$	$n = 1.0$	$m = -0.5$	$m = 0$	$m = 0.5$	$m = 1.0$
1.0	0.5642	0.8862	1.1284	0.5642	0.8863	1.1284	1.3294
0.9	0.5098	0.8014	1.0206	0.5082	0.7979	1.0159	1.1968
0.8	0.4603	0.7259	0.9250	0.4553	0.7127	0.9064	1.0672
0.7	0.4174	0.6629	0.8457	0.4114	0.6364	0.8058	0.9465
0.6	0.3832	0.6160	0.7877	0.3849	0.5790	0.7248	0.8258
0.5	0.3603	0.5890	0.7555	0.3812	0.5508	0.6765	0.7800
0.4	0.3506	0.5844	0.7522	0.3986	0.5548	0.6673	0.7588
0.3	0.3550	0.6026	0.7783	0.4315	0.5853	0.6930	0.7791
0.2	0.3732	0.6419	0.8314	0.4749	0.6350	0.7448	0.8313
0.1	0.4035	0.6991	0.9071	0.5257	0.6983	0.8154	0.9070
0.0	0.4438	0.7704	1.0000	0.5818	0.7715	0.8998	0.9999

$0 \leqslant n \leqslant 1$. At a given value of χ, as n increases the Nusselt number increases. It is also seen that the Nusselt number curve reaches a minimum value at a certain χ value between 0 and 1. This is due to the nature of the $Nu_x(Pe_x^{1/2}+Ra_x^{1/2})^{-1}$ vs χ plot and does not imply that the actual Nu_x value for mixed convection is smaller than that for pure forced or pure free convection. For example, consider the case of $n = 0$ and $\chi = 0.5$. If the Peclet number is taken as $Pe_x = 100$, the corresponding Rayleigh number can be found from the χ expression to be $Ra_x = 100$. Using the $-\theta'(\chi, 0)$ values listed in Table 1, the local Nusselt number Nu_x for mixed convection ($Pe_x = 100$, $Ra_x = 100$) is 7.206, but for pure forced convection ($Pe_x = 100$) and pure free convection ($Ra_x = 100$), the Nu_x values are found to be 5.642 and 4.438, respectively. From these results, it is obvious that the predicted value of local Nusselt number for mixed convection is higher than that for pure forced convection and pure free convection.

For practical purposes, correlation equations for the local Nusselt numbers were developed for pure forced convection, Nu_f, pure free convection, Nu_n, and mixed convection, Nu_x. The equations for Nu_f and Nu_n, which are valid for $0 \leqslant n \leqslant 1$ and with an error of less than 2%, are given by

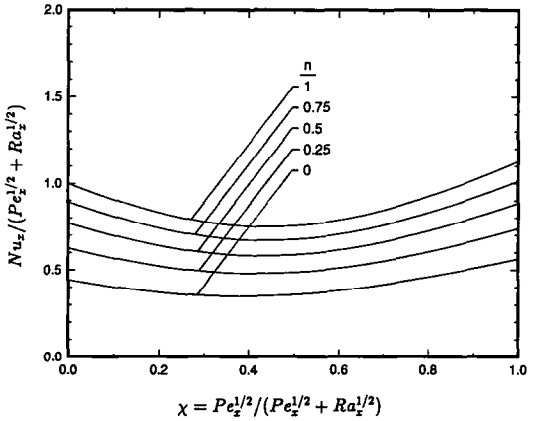

FIG. 3. Local Nusselt number at selected values of n (VWT case).

$$Nu_f = g_1(n)Pe_x^{1/2} \tag{29}$$

$$Nu_n = g_2(n)Ra_x^{1/2} \tag{30}$$

where

$$g_1(n) = 0.5650+0.7631n-0.2813n^2+0.0821n^3 \tag{31}$$

$$g_2(n) = 0.4457+0.8099n-0.3831n^2+0.1286n^3. \tag{32}$$

Following Churchill [13], the correlation equation for the local Nusselt number in mixed convection, Nu_x, can be expressed as

$$\left(\frac{Nu_x}{Nu_f}\right)^p = 1+\left(\frac{Nu_n}{Nu_f}\right)^p. \tag{33}$$

Substituting equations (29) and (30) into equation (33), the correlation equation for the local Nusselt number in terms of χ parameter can be presented by

$$\frac{Nu_x(Pe_x^{1/2}+Ra_x^{1/2})^{-1}}{g_1(n)} = \left\{\chi^p+\left[(1-\chi)\frac{g_2(n)}{g_1(n)}\right]^p\right\}^{1/p}. \tag{34}$$

The average Nusselt numbers for pure forced convection and pure free convection are found as

$$\overline{Nu_f} = 2g_1(n)Pe_L^{1/2} \tag{35}$$

$$\overline{Nu_n} = \frac{2}{n+1}g_2(n)Ra_L^{1/2} \tag{36}$$

where Pe_L and Ra_L are the values of Pe_x and Ra_x at $x = L$. The corresponding correlation equation for the average mixed convection Nusselt number $\overline{Nu}$ can be expressed as

$$\frac{\overline{Nu}(Pe_L^{1/2}+Ra_L^{1/2})^{-1}}{g_1(n)} = \left\{(2\chi_L)^p+\left[(1-\chi_L)\frac{2g_2(n)}{(n+1)g_1(n)}\right]^p\right\}^{1/p}. \tag{37}$$

When $p = 2$ is used, the maximum deviation

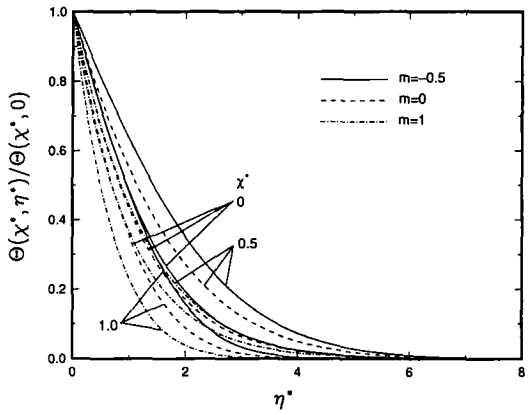

FIG. 4. Dimensionless temperature profiles at selected values of χ^* and m (VHF case).

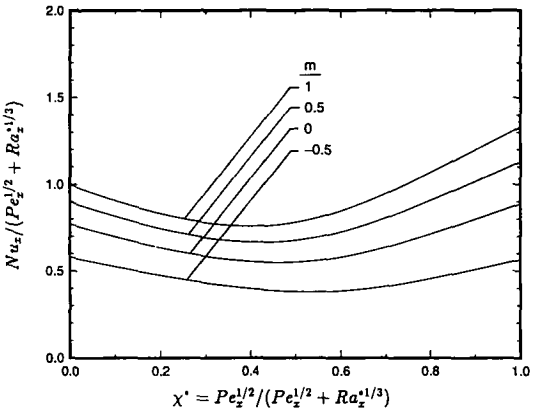

FIG. 6. Local Nusselt number at selected values of m (VHF case).

between the correlated results from equations (34) and (37) and the predicted results from equations (14) and (15) is about 0.4% for $0 \leqslant n \leqslant 1$ over the entire regime of mixed convection. However, this maximum deviation will increase to about 11% if $p = 3$ is used.

B. *Power-law variation of surface heat flux*

Figures 4 and 5 show, respectively, the dimensionless temperature profiles in terms of $\Theta(\chi^*, \eta^*)/\Theta(\chi^*, 0)$ and the dimensionless velocity profiles in terms of $F'(\chi^*, \eta^*)$ at selected values of χ^* for $-0.5 \leqslant m \leqslant 1$. The trends and behaviors of these curves are similar to those for the variable wall temperature case because the effects between the two cases are similar.

The values of $1/\Theta(\chi^*, 0)$ at different values of χ^* and m are also listed in Table 1. The local Nusselt number in terms of $Nu_x(Pe_x^{1/2}+Ra_x^{*1/3})^{-1}$, or $1/\Theta(\chi^*, 0)$, as a function of χ^* is illustrated in Fig. 6 for the exponent values $-0.5 \leqslant m \leqslant 1$. The behavior of the local Nusselt number curves is similar to that for the VWT case.

As in the VWT case, the local Nusselt number in terms of $Nu_x(Pe_x^{1/2}+Ra_x^{*1/3})^{-1}$ has a minimum value between $0 \leqslant \chi^* \leqslant 1$. However, the Nu_x value for mixed convection is actually higher than those for pure forced convection ($\chi^* = 1$) and pure free convection ($\chi^* = 0$). For example, for the case of $m = 0$ and $\chi^* = 0.5$ with $Pe_x = 100$, one finds $Ra_x^* = 1000$ and the Nu_x values for $\chi^* = 0$, 0.5, and 1.0 are, respectively, 7.715, 11.016, and 8.863 when use is made of the $1/\Theta(\chi^*, 0)$ values listed in Table 1.

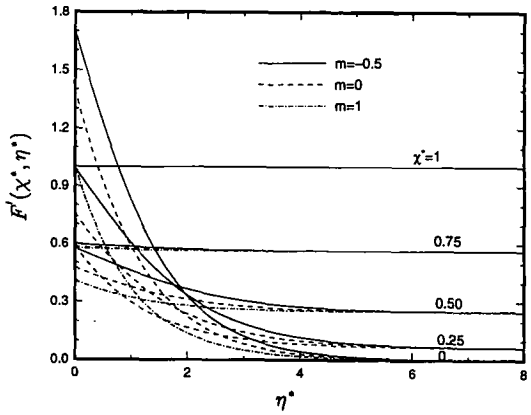

FIG. 5. Dimensionless velocity profiles $F'(\chi^*, \eta^*)$ at selected values of χ^* and m (VHF case).

The local Nusselt numbers for pure forced convection and pure free convection for the VHF case can be correlated by

$$Nu_f = g_3(m)Pe_x^{1/2} \tag{38}$$

$$Nu_n = g_4(m)Ra_x^{*1/3} \tag{39}$$

for $-0.5 \leqslant m \leqslant 1$, where

$$g_3(m) = 0.8864+0.5488m-0.1559m^2+0.0516m^3 \tag{40}$$

$$g_4(m) = 0.7718+0.3043m-0.1189m^2+0.0444m^3. \tag{41}$$

The above equations fit the computed results within an error of about 2%. The correlation equation for the local Nusselt number in terms of the χ^* parameter can be represented by

$$\frac{Nu_x(Pe_x^{1/2}+Ra_x^{*1/3})^{-1}}{g_3(m)} = \left\{\chi^{*p}+\left[(1-\chi^*)\frac{g_4(m)}{g_3(m)}\right]^p\right\}^{1/p}. \tag{42}$$

The average Nusselt numbers for pure forced convection, pure free convection, and mixed convection can be correlated, respectively, by the equations

$$\overline{Nu_f} = 2g_3(m)Pe_L^{1/2} \tag{43}$$

$$\overline{Nu_n} = \frac{3}{m+2}g_4(m)Ra_L^{*1/3} \tag{44}$$

$$\frac{\overline{Nu}(Pe_L^{1/2}+Ra_L^{*1/3})^{-1}}{g_3(m)} = \left\{(2\chi_L^*)^p + \left[(1-\chi_L^*)\frac{3g_4(m)}{(m+2)g_3(m)}\right]^p\right\}^{1/p} \quad (45)$$

where Pe_L and Ra_L^* are the values of Pe_x and Ra_x^* at $x = L$.

Again, the value of exponent p can be 2 or 3. When $p = 3$ is used, equations (42) and (45) are found to correlate very well with the predicted results from equations (26) and (27), with a maximum deviation of about 5% in the range of $-0.5 \leqslant m \leqslant 1$ over the entire regime of mixed convection. A choice of $p = 2$ will result in a maximum deviation of about 7%.

It should be mentioned that if the Peclet and Rayleigh numbers become sufficiently large, Darcy's model may not be acceptable, as discussed by Bejan and Poulikakos [14] for natural convection. However, according to the experimental work of Cheng *et al.* [15], the present results are expected to be valid for Rayleigh numbers less than 1000. The present results cover the special cases studied by Cheng [2] for $n = 0$, Cheng and Minkowycz [3] for $\chi = 0$, and Bejan [16] for $\chi = 1$ with $n = 0$ and $\chi^* = 1$ with $m = 0$.

CONCLUDING REMARKS

The problem of mixed convection from a vertical flat plate embedded in a porous medium is analyzed by introducing nonsimilarity parameters $\chi = [1+(Ra_x/Pe_x)^{1/2}]^{-1}$ and $\chi^* = [1+(Ra_x^*/Pe_x^{3/2})^{1/3}]^{-1}$ for the cases of power-law variation in wall temperature and surface heat flux, respectively. Temperature and velocity profiles are presented for the entire mixed convection regime ranging from pure forced convection ($\chi = 1$ ot $\chi^* = 1$) to pure free convection ($\chi = 0$ or $\chi^* = 0$). The local Nusselt number for the entire mixed convection regime at selected values of the exponent n or m are also presented. In addition, general correlation equations for the local and average Nusselt numbers are provided. The maximum deviation between the correlated and the predicted mixed convection Nusselt numbers is about 5% for both heating conditions.

Acknowledgement—The present study was supported in part by a grant from the University of Missouri (Weldon Spring/Chen/91-92).

REFERENCES

1. P. Cheng, Similarity solutions for mixed convection from horizontal impermeable surfaces in saturated porous media, *Int. J. Heat Mass Transfer* **20,** 893–898 (1977).
2. P. Cheng, Combined free and forced convection flow about inclined surfaces in porous media, *Int. J. Heat Mass Transfer* **20,** 807–814 (1977).
3. P. Cheng and W. J. Minkowycz, Free convection about a vertical flat plate embedded in a porous medium with application to heat transfer from a dike, *J. geophys. Res.* **82,** 2040–2044 (1977).
4. W. J. Minkowycz and P. Cheng, Free convection about a vertical cylinder embedded in a porous medium, *Int. J. Heat Mass Transfer* **19,** 805–813 (1976).
5. P. Cheng and I-Dee Chang, Buoyancy induced flows in a saturated porous medium adjacent to impermeable horizontal surfaces, *Int. J. Heat Mass Transfer* **19,** 1267–1272 (1976).
6. J. T. Hong, Y. Yamada and C. L. Tien, Effects of non-Darcian and nonuniform porosity on vertical-plate natural convection in porous media, *J. Heat Transfer* **109,** 356–362 (1987).
7. C. T. Hsu and P. Cheng, The Brinkman model for natural convection about a semi-infinite vertical flat plate in a porous medium, *Int. J. Heat Mass Transfer* **28,** 683–697 (1985).
8. A. Nakayama and H. Koyama, A general similarity transformation for combined free and forced convection flows within a fluid-saturated porous medium, *J. Heat Transfer* **109,** 1041–1045 (1987).
9. A. Nakayama and I. Pop, A unified similarity transformation for free, forced and mixed convection in Darcy and non-Darcy porous media, *Int. J. Heat Mass Transfer* **34,** 357–367 (1991).
10. W. J. Minkowycz, P. Cheng and C. H. Chang, Mixed convection about a non-isothermal cylinder and sphere in a porous medium, *Numer. Heat Transfer* **8,** 349–359 (1985).
11. J. C. Hsieh, T. S. Chen and B. F. Armaly, Nonsimilarity solutions for mixed convection from vertical surfaces in a porous medium: variable surface temperature or heat flux, *Int. J. Heat Mass Transfer* **36,** 1485–1493 (1993).
12. T. Cebeci and P. Bradshaw, *Momentum Transfer in Boundary Layers*, Chaps. 7–8. Hemisphere, Washington, DC (1977).
13. S. W. Churchill, A comprehensive correlating equation for laminar assisting, forced and free convection, *A.I.Ch.E. Jl* **23,** 10–16 (1977).
14. A. Bejan and D. Poulikakos, The nonDarcy regime for vertical boundary layer natural convection in a porous medium, *Int. J. Heat Mass Transfer* **27,** 717–722 (1984).
15. P. Cheng, C. L. Ali and A. K. Verma, An experimental study of non-Darcian effects in free convection in a saturated porous medium, *Lett. Heat Mass Transfer* **8,** 261–265 (1981).
16. A. Bejan, *Convection Heat Transfer*, Chap. 10, pp. 355–358. Wiley, New York (1984).